Development of a CFD model for simulating a floating solar platform in irregular wave regimes

Development of a CFD model for Simulating a Floating Solar Platform in Irregular Wave Regimes

G. Baruah, M. Karimirad, D. Friel and P. Mackinnon
School of Natural and Built Environment, Queen's University Belfast, Belfast, United Kingdom.

A. Abbasnia
Centre for Marine Technology and Ocean Engineering (CENTEC), Instituto Superior Técnico, Universidade de Lisboa, Lisbon, Portugal

N. Sarmah
Department of Energy, Tezpur University, Napaam, Tezpur, Assam, India.

ABSTRACT: In this paper a RANS (Reynolds-averaged Navier–Stokes) model is developed to determine the floating solar platform response in random wave regimes. The model takes advantage of the finite volume solver and the Volume of Fluid method (VoF) to solve the two-phase fluid flow which is enhanced by the k-ω SST model. Initially the model emerged for simulation of a floating solar platform in regular waves and mesh convergence and stability analysis were carried out to assess the accuracy of the model. The numerical model is fostered currently for irregular waves and the performance of the numerical model is investigated for frequency ranges of the JONSWAP spectrum. A set of experimental data is compared with the numerical results for verification and the range of validity of the model is outlined. The responses show the presence of higher order harmonics, and, with further adjustments, the model can be utilized to study steeper non-linear waves. Thus, a useful approach in studying the responses of the solar platform and its sensitivity for irregular waves can be achieved which could be crucial to identify resonance and design of solar platforms along with mooring lines.

1 INTRODUCTION

There has been significant growth in floating solar photovoltaics (FPV) over the past few decades, with a total installed capacity of 1314 MWp and projections of 4600 MWp by 2022. (Masson, G., et.al., 2019). The technology has been propounded as a functional alternative to ground-mounted installations. Floating photovoltaics have not only mitigated the use of land resources but also efficiency losses through natural cooling effects and decarbonization objectives (Oliveira-pinto and Stokkermans, 2020). FPV systems are essentially an integrated combination of floaters, a mooring system, PV modules, cabling, and connectors (Sahu et al., 2016), as illustrated in Figure 1:

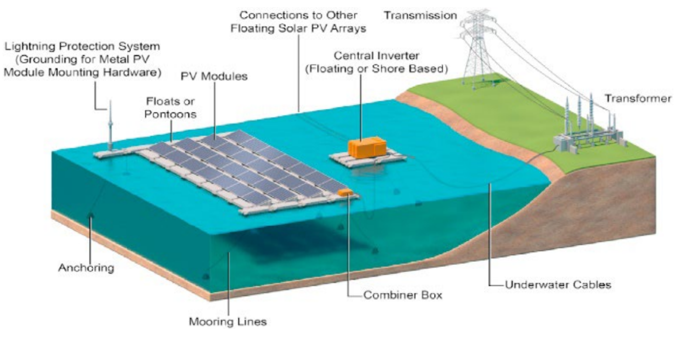

Figure 1. Schematic of a Floating Photovoltaic System (Lee et.al., 2020)

The major challenges to the sustainability of FPV systems both inland and offshore, are the survivability of the platform upon the environmental loads such as wind, waves, and currents. Thus, an accurate estimation of the responses is essential in the basic design of the platforms. Previous studies on FPV installations and load estimations relate to the numerous technologies implemented and the approaches to environmental load estimations (Friel et. al., 2019).

Studies on wind interactions with floating platforms document the effect of wind loadings with inclination angles, panel width, and tracking (Redón-Santafé et. al., 2014; Rosa-Clot et.al., 2018) and load calculations for even extreme wind loads (Siribodhi and Bunyawanichakul, 2019). In another study, both the effects of wind and wave loads were investigated on a thin-film solar panel, carried out as a Computational Fluid Dynamics (CFD) analysis using Solidworks (Trapani and Miller, 2016).

Although most of the prior studies involved regular wave interactions with solar platforms, nonlinear analysis of an FPV platform under incident irregular waves was investigated by Friel et al. (2020) where, the dynamics of a moored double-hulled platform were considered, and spectral analysis was conducted to study the nonlinearities of the wave structure interaction.

Hydrodynamic analysis for irregular wave interactions with floating objects, in general, has been previously documented involving Ocean Wave Energy Surge Converters (OWSC) and other ocean energy devices. This involved model experiments for both regular and irregular waves to analyze the efficiency and performance of OWSC models which were compared with CFD results using OpenFOAM (Vyzikas et al., 2017). Computations of wave elevation for OWSC were done and compared to experimental data using 1-D models and a 2-D nonlinear numerical wave tank (Gervelas et al., 2011; Koo and Kim, 2012) for irregular waves. Commonly a 2-D numerical wave tank based on potential theory (Koo and Kim, 2007; Abbasnia and Guedes Soares, 2018; Abbasnia et al., 2021) as well as viscous flow (Li and Lin, 2010; Li and Lin, 2012) has been utilized to demonstrate the capability of numerical models to solve the wave-body problem. To compute the response dynamics of the irregular wave interactions, the implementation of high-fidelity software for the development of a numerical model is requisite.

The open-source software OpenFOAM, with its vast repository of solvers, has demonstrated its validity to develop numerical models for wave-body interaction problems. OpenFOAM was used to study the effects of different incident waves on a novel Oscillating Water Column (OWC) (Masoomi et. al., 2021) wherein the Volume of Fluid method (VOF) was used, and the numerical results were verified with experimental data. Similarly, wave structure interaction between a cylinder and incident waves was investigated by Hu et al. (2019). Different approaches for wave generation and wave absorption have been explored in OpenFOAM to retain the open-sea condition during the simulation. Wave propagation using relaxation zones and active wave generation and absorption boundary conditions have been successfully implemented in prior studies (Jacobsen et. al., 2012; Higuera et al., 2013).

The current paper outlines the development of a numerical wave tank in OpenFOAM for a floating solar platform structure under a range of frequencies for irregular waves. It is based on the viscous model developed to study the wave structure interactions between the platform and monochromatic waves. (Baruah et al. (2022). Here, the interactions between non-linear monochromatic waves and the twin-cylinder platform are simulated to validate the model with experimental data, where the response in axial force is compared. The model is developed further to study the interactions between irregular waves with the platform. The JONSWAP wave spectrum was used in the OpenFOAM model as the input. Spectrum comparison was done to check the accuracy of wave realization from OpenFOAM. Spectral analysis of the time domain responses of the platform is conducted and compared to the experimental data. The comparisons demonstrate the consistency between the numerical results and the experiments and the validity of the model for capturing the dynamics of irregular waves is shown. The paper provides a useful study for the response analysis of floating solar platforms and their sensitivity to input signal frequencies when subjected to incident non-linear irregular waves. The analysis in this paper is limited to shallow regular and irregular waves based on the JONSWAP spectrum. The results show a good capture of the responses and a fair degree of conformance with the experimental results. They also highlight the presence of higher-order harmonics in the responses. With further adjustments to the model, a comprehensive approach to studying steeper waves can be achieved which could be crucial to understanding resonance and turbulence effects with increasing non-linearity in such solar platforms.

2. NUMERICAL MODEL DEVELOPMENT

2.1 Governing equations and numerical approach

For the wave structure interaction analysis, a two-dimensional computational domain was developed based on the schematic for the experimental system illustrated in Figure 2.

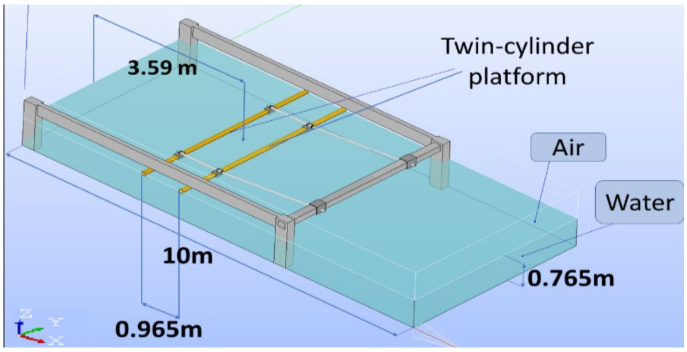

Figure 2: 3D Schematic for the twin-cylinder platform in the wave tank

A global right-hand oriented Cartesian coordinates system (Oxz) is placed at the bottom of the numerical wave tank and the x- and the z-axis is oriented horizontally and vertically respectively, as shown in Figure 2. The domain utilizes the Reynolds Average Navier-Stokes (RANS) equations with the incompressibility assumptions for the Newtonian fluids air and water. They are described by the following equations:

$$\vec{\nabla} . \vec{U} = 0$$
$$\frac{\partial \vec{U}}{\partial t} + \vec{U} . \nabla \vec{U} = - \frac{1}{\rho} \overrightarrow{\nabla p} + g + \vec{\nabla} . \left[\left(\nu + \nu_t \right) \left(\nabla \vec{U} + \nabla \vec{U}^T \right) \right] \quad (1)$$

where g is the acceleration due to gravity and p represents the fluid pressure. The velocity vector is denoted as $\vec{U} = \left(u_x \; u_y \; u_z \right)$ and $\vec{U}^T$ represents the transient component of the velocity. t is the time. and fluid density is denoted by ρ.

The kinematic and turbulent viscosities are denoted by υ and υ_t. The *SST* $k-\omega$ model (Menter, 1994) is used to estimate the turbulent viscosity. The effective capture of the air-water interface is achieved by implementing the Volume of Fluid (VoF) method (Hirt and Nichols, 1981), based on a volume fraction (α). This value is 0 for a completely dry cell and 1 for a completely wet cell and between 0 and 1 for one containing both water and air. A discrete integration of α determines the free surface position as follows:

$$z_{water\ level} = \sum_{i=0}^{n-1} \alpha_i \left(z_{i+1} - z_i \right) \quad (2)$$

where the z-direction is the vertical line divided by n parts, over which the integration is performed (Devolder et. al., 2017).

The solution of the RANS equation (Equation 1) is obtained implicitly by the Finite Volume Method (FVM). The pressure and velocity of the entire domain are integrated using the PIMPLE algorithm, which is essentially a combination of the Pressure Implicit with Splitting Operator (PISO) (Issa, 1986) with the Semi-Implicit Method for Pressure-Linked Equations (SIMPLE) algorithm. The Total Variation Diminishing (TVD) scheme is employed to discretize the diffusion terms by way of a second-order central difference.

OpenFOAM has a vast repository of solvers which can be utilized to achieve numerical solutions. The interFOAM solver which implements the discussed approach is used in the present paper. Implementation of an active wave generation at the inlet boundary and an active wave absorption at the outlet is employed (Higuera et. al., 2013) to dampen the wave reflection at the outlet. The effect of air velocity is not considered for the domain. The spatial discretization of the domain is achieved by employing the built-in OpenFoam utility snappyHexMesh, where a hexagonal mesh type is generated. Table 1 denotes the Boundary Conditions (BC) defined for the simulation and Figure 3 represents the 2-D discretized domain for the study.

Table 1. Boundary conditions of the computational domain

BC	Inlet	Outlet
p	*fixedFluxPressure*	*fixedFluxPressure*
$\vec{U}$	*WaveVelocity*	*WaveVelocity*
k	*fixedValue*	*inletOutlet*
ω	*fixedValue*	*inletOutlet*
ν_t	*fixedValue*	*ZeroGradient*
Γ	*Waves InletAlpha*	*ZeroGradient*
BC	**Top**	**Bottom**
p	*totalPressure*	*fixedFluxPressure*
$\vec{U}$	*pressureInletOutletVelocity*	*fixedValue*
k	*inletOutlet*	*kqRWallFunction*
ω	*inletOutlet*	*omegaWallFunction*
ν_t	*ZeroGradient*	*nutkRoughWallFunction*
Γ	*inletOutlet*	*ZeroGradient*
BC	**Floating solar platform**	
p	*fixedFluxPressure*	
$\vec{U}$	*fixedValue* *	
k	*kqRWallFunction*	
ω	*omegaWallFunction*	
ν_t	*nutkRoughWallFunction*	
Γ	*ZeroGradient*	

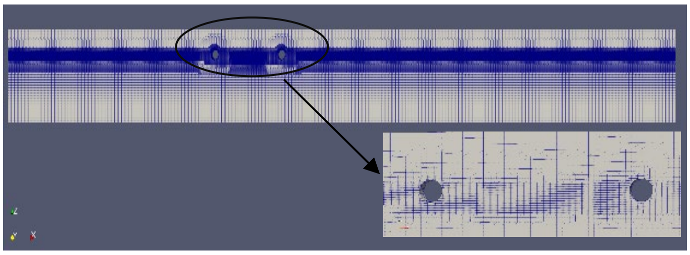

Figure 3. Spatial discretized computational domain

2.2 Irregular wave generation

To realize the open sea condition for irregular waves, a spectrum is generated using MATLAB through the Wave Analysis for Fatigue and Oceanography (WAFO) toolbox (WAFO-group, 2000). For the current paper, a JONSWAP spectrum is generated of a specific peak period and significant wave height. The IHFOAM toolbox developed by Higuera et. al., (2013) is utilized to define the wave properties as input to OpenFOAM. Wave period and wave height are two of the inputs calculated using MATLAB. A random function is used to define a random wave phase and the wave direction is defined in a way to provide a unidirectional input to OpenFOAM. The time-domain results from OpenFOAM are converted to the frequency domain using Fast Fourier Transform in WAFO to conduct the spectral analysis.

3. NUMERICAL APPLICATIONS

3.1 Mesh convergence test

The mesh convergence test for the domain is carried out using nonlinear regular incident waves in the absence of an object. Second-order Stokes waves were chosen for the simulation, determined by the characteristics of the specified waves and their position in the validation range of available wave theories (Le Méhauté, 1976). The convergence test has been discussed in detail by Baruah et. al. (2022) where the error analysis for different mesh sizes was considered. Using the same approach, mesh convergence was carried out. A decrease in accuracy of the model was observed for high steepness waves with the effect of increasing non-linearity attributed to them. The simulations were carried out using the QUB (Queen's University Belfast) Kelvin2 Scalable High-Performance Computer (HPC) and the specifications of the machine include dual 64-Core AMD EPYC 7702 CPU 2-3.35 GHz, RAM 12 GB.

3.2 Dynamic responses of the twin-cylinder floating platform with monochromatic waves

A set of experimental data was obtained for the interaction of a twin-cylinder platform and incident waves in the hydraulic lab of Queen's University Belfast. The incident waves considered were a set of monochromatic and irregular waves generated by a 6-paddle wavemaker. The diameter of each cylinder is taken as 0.11m. The centre of the first cylinder from the wavemaker was located in still water at 5m with a water depth of 0.765m. The mesh sizes for the domain are considered as follows:

$N_x = 1000$, $N_z = 100$ where N_x and N_z are the number of cells in the x- and z-directions respectively.

The floating platform response dynamics in heave and pitch for three distinct sea states were studied by Baruah et.al.,2020 where a comparison of the same was done with experimental data. Reasonable conformance was reported for the responses with deviations mainly due to the asymmetric trend of the experimental results. Figure 4 and Figure 5 illustrate the time series results in heave and pitch for one of the sea states considered.

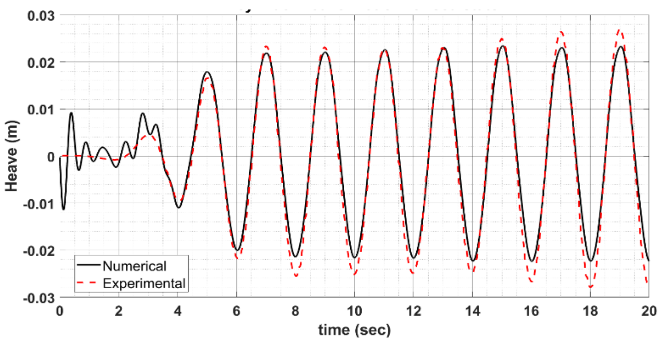

Figure 4. Time Series of Heave Motion for A Twin Cylinder Floating Solar Platform in Waves. (Baruah et. al., 2020)

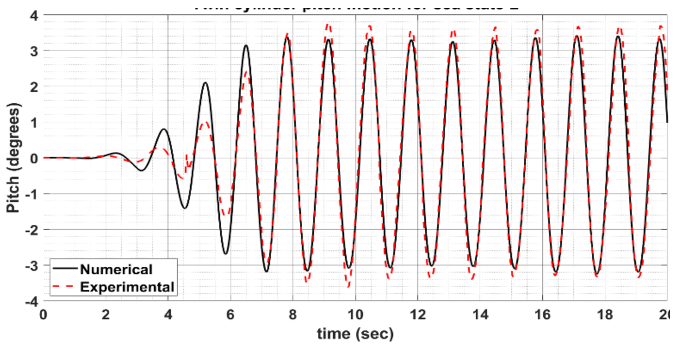

Figure 5. Time Series of Pitch Motion for a Twin Cylinder Floating Solar Platform in Waves. (Baruah et.al, 2020)

The total axial forces on the floating platform encountered in the surge axis (X-axis) have been investigated here. To accomplish the matter, two load cells were set up on the cylinders in the physical wave tank to record the instantaneous axial force and the filtered measurements were compared with the results of the numerical wave tank. For simplicity, the connection between the cylinders is considered massless. The sea states considered for the analysis have been specified in Table 2.

Table 2. Wave characteristics of the three monochromatic sea states.

Sea state	Wave height (*m*)	Wavenumber (m^{-1})	Wave steepness
1	0.056	1.31	0.011
2	0.063	2.38	0.024
3	0.05	4.0	0.031

The centres of the two cylinders of the platform are spaced 0.965m apart. The centre of mass of the system is defined at the mid-point of the system. The cylinders considered for the study are made of Polyvinyl Chloride (PVC) and placed in a half-submerged condition inside the tank. Figure 6 illustrates the arrangement for the platform and the physical properties which are summarized in Table 3:

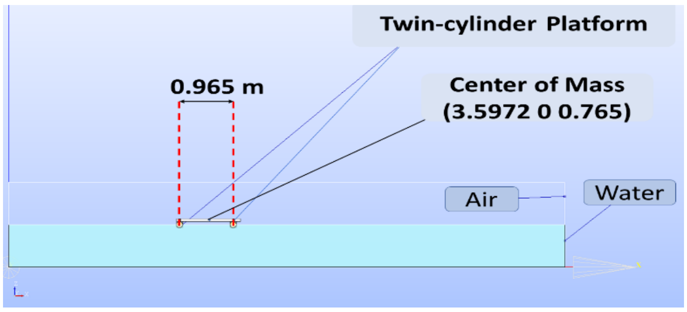

Figure 6: Twin-cylinder arrangement for the numerical and experimental estimations.

Table 3. Physical properties of the platform

Property	Value
Mass	0.94 kg
Density	1330 kg/m^3
Moment of Inertia(Iyy)	0.235 m^2-kg
Center of mass co-ordinates	(3.5972, 0, 0.765)

To compute the axial forces, the OpenFOAM function object ‘forcesIncompressible’ was used. The results from OpenFOAM were then compared with the experimental data. For the axial force over-plots, a normalized time (t/T) was used, where t is the simulation time and T is the wave period of the sea states. Figure 7 illustrates the normalized time series of axial force for the floating platform. The three sea states have different celerity and as they propagate to interact with the platform, the states with shorter wavelengths take more time to reach the first cylinder. Thus, a longer delay in dynamic response is observed for the shorter wavelengths.

The axial over-plots indicate an increasing deviation with steeper waves. This could be due to the increase in turbulence in the gap between the cylinders. However, it could be seen that for Sea State 3 there is an overestimation of the numerical results with lesser deviation. Inaccuracies and errors in the experimentation cannot be ruled out, as highlighted by the consistency of the response profiles from the numerical results as against the experimental ones.

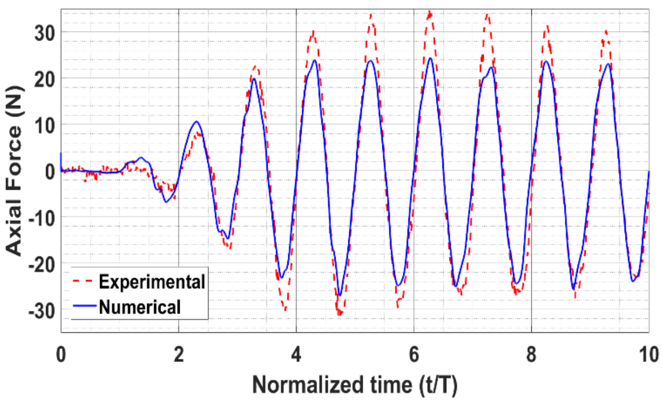

a. Sea State 1

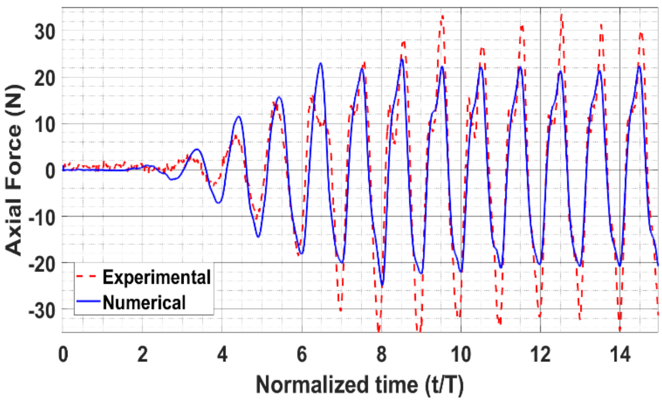

a. Sea state 2

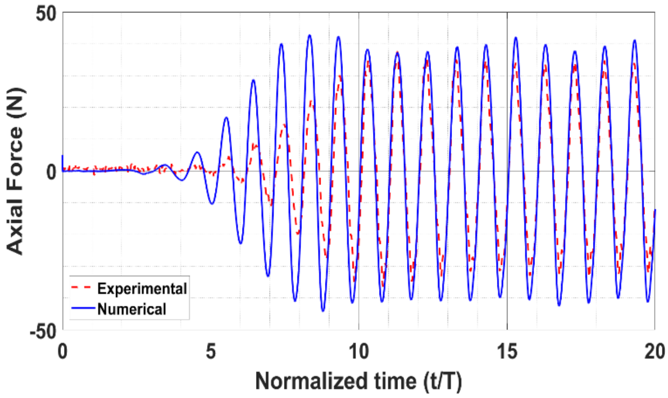

b. Sea state 3

Figure 7. Normalized Time Series of Axial Force for a Twin Cylinder Floating Solar Platform in Waves

3.3 Irregular wave interactions with twin-*cylinder floating platform*

Three irregular sea states based on JONSWAP characteristics are specified in OpenFOAM, as denoted in Table 4. The other parameters were kept the same as in the regular case.

Table 4. Incident irregular wave characteristics

Sea state	Significant Wave height (*m*)	Peak Period (sec)
1	0.025	2
2	0.05	1.33
3	0.075	1

The accuracy of the wave realization by the software from its input is crucial for the consistency of the model. Hence, the characteristics of the wave generated by OpenFOAM are first compared with the input wave properties. The simulations are run without the platform and the time series obtained is then converted to its frequency domain. The significant wave heights and peak periods obtained from the spectra are compared. This is done using WAFO. Figure 8 shows the over-plots of the input and output wave spectra from OpenFOAM.

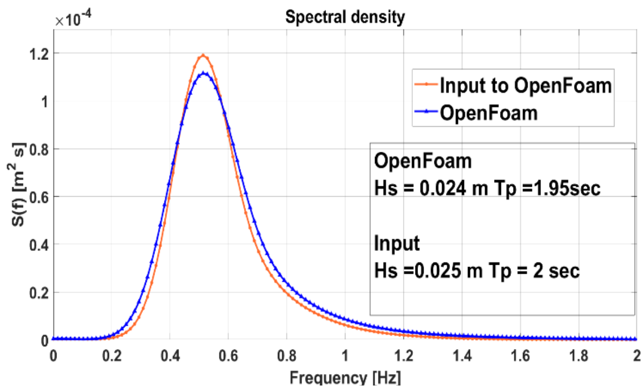

a. Sea state 1

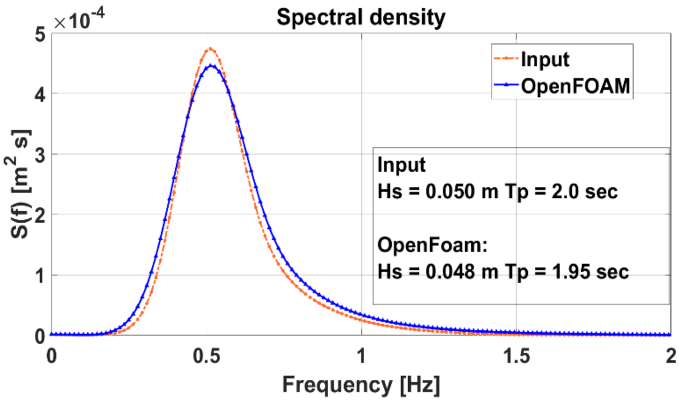

b. Sea state 2

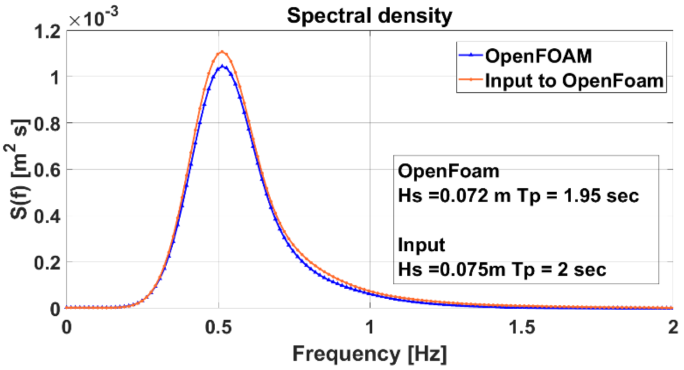

c. Sea state 3

Figure 8. Wave spectra comparison between the input to OpenFOAM solver and the output time series from OpenFOAM

The result from the plots shows reasonable conformance between the input and the OpenFOAM output. This is further highlighted by the comparison between the computed wave properties from the spectra where the differences in significant wave height are within 0.003m for the steepest waves, Sea State 3. For the peak period, the differences are within 0.05 seconds.

With an accurate realization of the irregular wave input, the twin-cylinder platform is then subjected to the specified three irregular sea states to obtain the time series of the dynamic responses. Fast Fourier Transform (FFT) is performed using WAFO to obtain the spectrum and then compared with the experimental spectrum.

The FFT performed on the signals can however lead to spectral leakage resulting in a smeared spectrum. These effects can be minimized by using a process called windowing. One such function is the Parzen window (Parzen, E., 1962), a non-parametric approach to estimating continuous density function from data using a mix of different continuous distributions called 'kernels'. The biggest advantage of this window is that it can be applied to the data from any distribution. Also, theoretically, it can be shown to converge when the sample size is very large. The critical parameter here is the window length, which is difficult to choose. A large bandwidth will oversmooth the density and mask the structure in the data while a small bandwidth will yield a density estimate that is spiky and very hard to interpret. The best practice is to choose different window widths and analyze the best performance of the derived classifier. The rule of thumb is to assume the shrinkage of the optimal window with an increase in sample size. Here, the bandwidth window (Bw) through a trial-and-error process is selected and kept the same for the experimental data as well.

The simulations for the three sea states were run for 50 seconds. Figure 9 shows the free surface dynamics of the three sea states. The capture of the platform interactions with the incident waves at different time instances is illustrated in Figure 10. The heaving and pitching of the platform can be visualized.

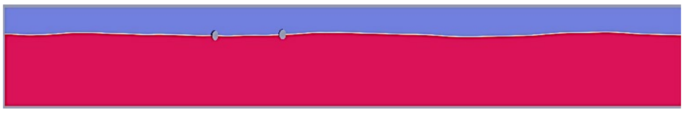

a. Sea state 1

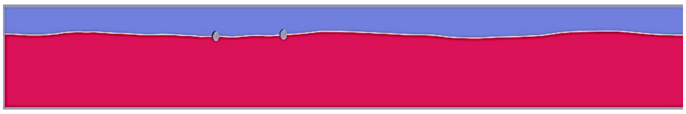

b. Sea State 2

c. Sea state 3

Figure 9. Normalized Time Series of Axial Force for a Twin Cylinder Floating Platform in Waves

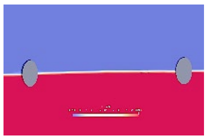

(a)

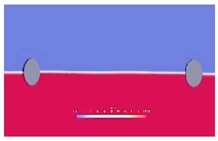

(b)

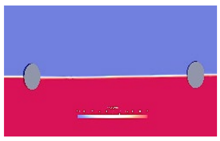

(c)

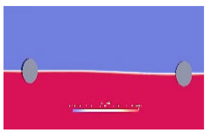

(d)

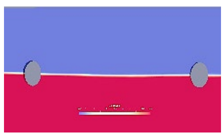

(e)

Figure 10. Snapshot of the twin-cylinder wave interactions at times (a) 10 sec (b) 20 sec (c) 30 sec (d) 40 sec and (e) 50 sec for Sea State-1

Comparative spectral analysis of the time series obtained from OpenFOAM is carried out with the experimental spectrum for heave, pitch, and axial force. The bandwidth window (Bw) for the Parzen filter used for both the experimental and numerical spectrum was kept at 0.245 Hz. Figure 11, Figure 12, and Figure 13 show the over plots of the numerical and the experimental results.

The results from the analysis show a close agreement of both the experimental and numerical responses with the input frequency of 0.5 Hz, which highlights the consistency of the model in capturing the dynamic response. The heave and pitch spectral responses show an increasing underestimation of the numerical results with the experimental data following a similar trend to the regular wave results. The increasing steepness of the waves and the associated non-linearity could be the cause of the deviations. The axial force responses indicate the presence of a second-order harmonic at 1.2 Hz along with the first-order harmonic response at 0.5 Hz. The heave responses suggest the presence of second-order harmonics at 1.15 Hz. The magnitude of the second harmonic is considerably lower than the first, however, this difference is less pronounced for the experimental results. The three sea states considered for the study have the same peak period of 2 seconds with different significant wave heights. The consistency of the harmonics for each of the three sea states for heave and axial forces highlights the accuracy of the model. The numerical responses also show a consistent trend with the increasing steepness of the waves. The experimental responses however do not conform to such a consistent trend.

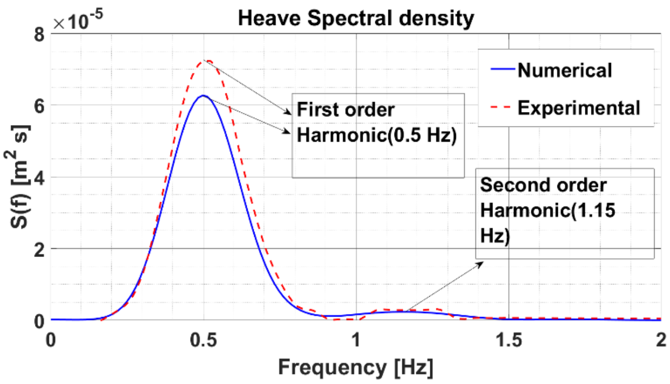

a. Sea state 1

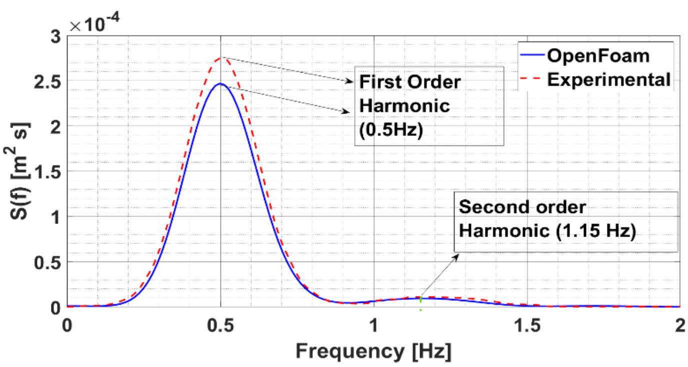

b. Sea state 2

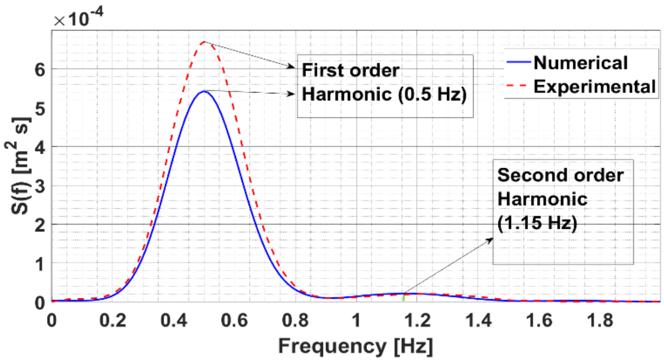

c. Sea state 3

Figure 11. Spectral analysis of Heave motion for a Twin Cylinder Floating Solar Platform in Irregular Waves

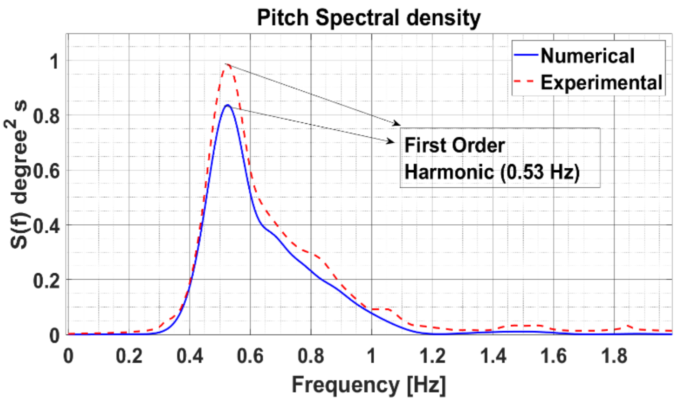

a. Sea state 1

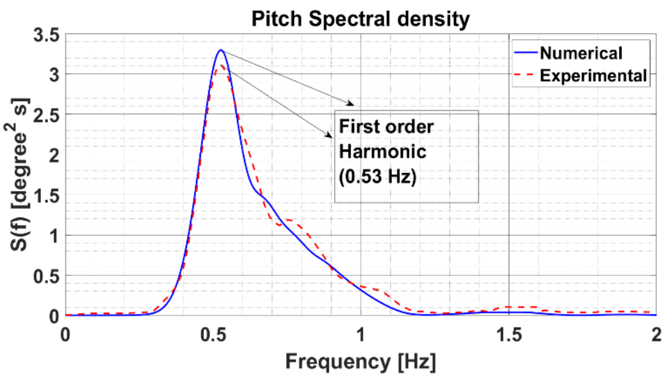

b. Sea state 3

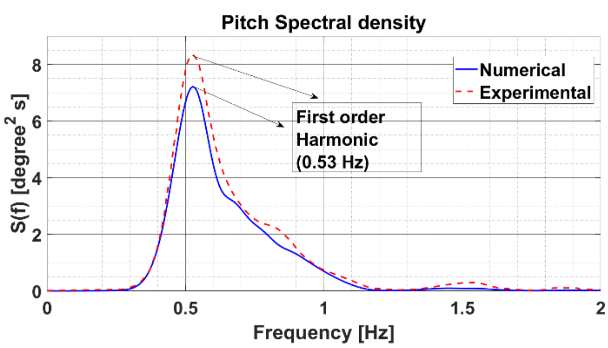

c. Sea state 3

Figure 12. Spectral analysis of Pitch motion for a Twin Cylinder Floating Solar Platform in Irregular Waves

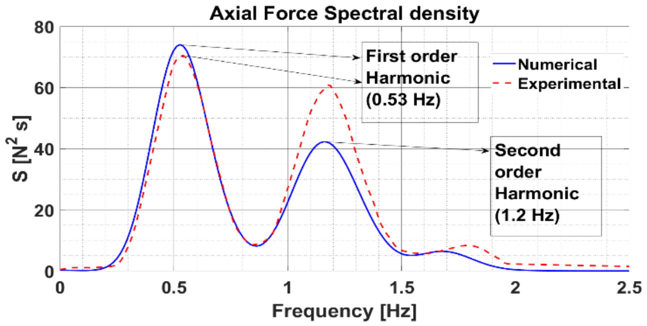

a. Sea state 1

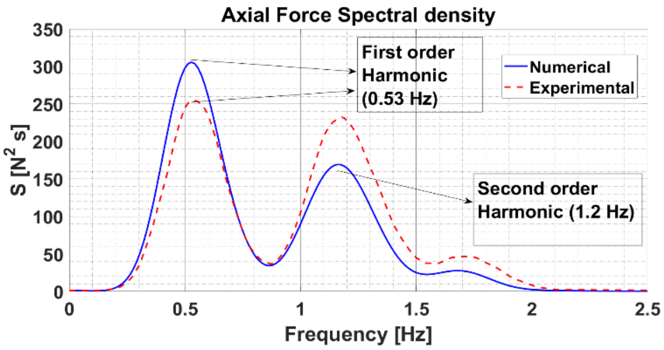

b. Sea state 2

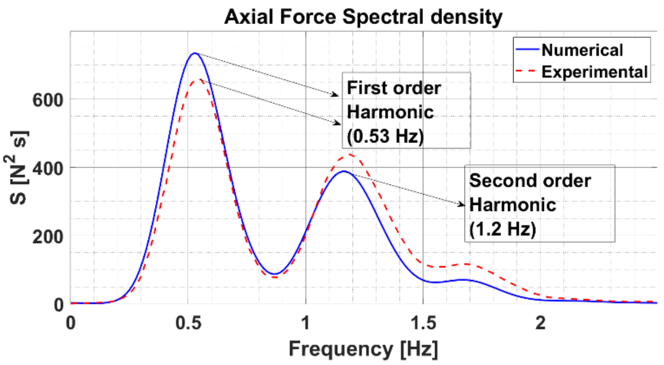

c. Sea state 3

Figure 13. Spectral analysis of Axial Forces for a Twin Cylinder Floating Solar Platform in Irregular Waves

4. CONCLUSION

A numerical model based on viscous flow was developed to capture the dynamic responses of a floating solar platform subjected to a set of nonlinear incident waves. The incident waves were both monochromatic and irregular. A finite volume solver to compute the RANS equations was utilized for the k-ω SST turbulence model. The interface capture was done using a Volume of Fluid approach. Mesh convergence was performed for the model with agreeable results. A twin-cylinder arrangement with a gap was considered as the floating platform. The 2-D discretized domain developed was then subjected to a range of incident monochromatic waves. The dynamic responses for the floating platform were evaluated for heave and pitch motion. Axial forces were also computed for the platform.

For validation, a set of experiments were performed in the wave tank of the Hydraulics Lab at Queen's University Belfast for a range of regular and irregular waves (Friel et. al., 2019). These were then compared with the numerical results. Acceptable conformance was found between the heave and pitch motions for all sea states. The deviation of the results was mainly due to a consistent asymmetry of the experimental results as well as experimental inaccuracies and unavoidable errors. The trend in increasing deviation with steepness was also observed. The model in this paper has been used to investigate shallower wave conditions with steepness values limited to 0.0517 for a water depth of 0.765m. This is because the method of dynamic capture for the platform is achieved through prescribed mesh motion in the OpenFOAM solver. This approach however results in divergence for high mesh deformation conditions. To investigate steeper wave conditions, an overset mesh approach will be considered in the future,

The floating platform was then subjected to a range of incident irregular waves realized in OpenFOAM. JONSWAP waves of specific peak period and significant wave height were generated using the WAFO toolbox in MATLAB and utilized as the input to OpenFOAM. The dynamic responses in heave and pitch were obtained along with the computation of the axial forces. Spectral analysis of the experimental and numerical data showed good agreement in terms of wave realization with the input. The axial force and heave response results highlighted the presence of higher-order harmonics which can be useful to determine the susceptibility of the system to resonant excitation. The numerical model demonstrated a better consistency in its capture of the responses than the experimental results.

The results presented in the paper could be a useful study in the sensitivity of floating solar platforms subjected to random open sea conditions. The accuracy in the irregular wave realization (deviations within 0.003 m in significant wave height and 0.05 seconds in peak period) and the consistent conformity with the experimental results suggests a useful approach to understanding the dynamic responses. The presence of higher-order harmonics (consistent estimations of harmonics at 0.5 and 1.15 Hz in heave, 0.53 Hz, and 1.2 Hz for axial forces) could be useful to identify the resonance susceptibility of the platforms, with the current work ongoing to correctly ascertain the natural frequencies and identify the possibility of resonant excitations.

ACKNOWLEDGEMENTS

The authors would like to thank Queen's University Belfast and Tezpur University for providing grants and access to the necessary resources. This includes access to the Kelvin2 High-Performance Computing (HPC) and Research Data Storage environment resources to carry out the simulations.

REFERENCES

Masson, G., et.al. (2019) 'Snapshot of Global PV Markets Strategic PV Analysis and Outreach', *IEA*., accessed on 10/04/2022.

Oliveira-Pinto, S., Stokkermans J. (2020) 'Assessment of the potential of different floating solar technologies - Overview and analysis of different case studies', *Energy Convers. Management,* 211, 112747.

Sahu, A., et. al. (2016) 'Floating photovoltaic power plant: A review', *Renew. Sust. Energy. Rev,* 66, pp. 815–824.

Lee, N., et.al. (2020) 'Hybrid floating solar photovoltaics-hydropower systems: Benefits and global assessment of technical potential', *Renewable Energy*, 162, pp. 1415-1427.

Friel, D., et. al., (2019), 'A review of floating photovoltaic design concepts and installed variations', *4th International Conference on Offshore Renewable Energy. CORE2019 proceedings*, ISBN 978-1-9996144-7-8, Glasgow: ASRA-Net Ltd, UK.

Santafé, M.R., et.al. (2014) 'Theoretical and experimental analysis of a floating photovoltaic cover for water irrigation reservoirs', *Energy*, 67, pp. 246–255.

Siribodhi, P., and Bunyawanichakul, P. (2019) 'Study and Evaluation of a Solar Floating Traction under Severe Wind Conditions', *IOP Conference Series: Materials Science and Engineering,* 642(1), 012003.

Trapani, K., and Millar, D. (2016) 'Hydrodynamic Overview of Flexible Floating Thin Film PV Arrays, *Offshore Energy and Storage Symposium*, *Malta.*

Friel, D., et.al. (2019) 'Hydrodynamic investigation of design parameters for a cylindrical type of floating solar system, *Developments in Renewable Energies Offshore – Guedes Soares (Ed.) Taylor & Francis Group, London,* ISBN 978-0-367-68131-9.

Vyzikas, T., et.al. (2017) 'Experimental investigation of different geometries of fixed oscillating water column devices', *Renew. Energy*, 104, pp. 248–258.

Gervelas, R., et.al. (2011) 'A time-domain simulator for an oscillating water column in irregular waves at model scale', *Ocean Eng*., 38, pp. 1007–1013.

Koo,W., and Kim, M.H. (2012) 'A time-domain simulation of an oscillating water column with irregular waves', *Ocean. Syst. Eng.*, 2, pp. 147–158.

Koo, W.C. and Kim, M.H. (2007) 'Fully non-linear wave body interactions with surface piercing bodies', *Ocean Eng*., 34, pp. 1000–1012.

Abbasnia, A. and Soares G. (2018) 'Fully nonlinear simulation of wave interaction with a cylindrical wave energy converter in a numerical wave tank', *Ocean Engineering*, 152(4), pp. 210-222.

Abbasnia,A., et al. (2021) 'Adaptive fully nonlinear potential model for the free surface under compressible air pressure of oscillating water column devices', *Engineering Analysis with Boundary Elements*, 133(4), pp. 153-164.

Li, Y., and Lin, M. (2010) 'Wave body interactions for a surface piercing body in water of finite depth', *J. Hydrodyn. Ser.,* B22(6), pp. 745–752.

Li, Y., and Lin, M. (2012) 'Regular and irregular wave impacts on floating body', *Ocean Engineering*, 42, pp. 93–101.

Masoomi, M., et.al. (2021) 'Efficiency Assessment of an Amended Oscillating Water Column Using OpenFOAM', *Sustainability,* 13, *5633*.

Hu, Z.Z., et.al. (2016), 'A Numerical wave tank study of extreme waves and wave-structure interaction using OpenFOAM®', *Ocean Eng.,* 126, pp. 329–342.

Jacobsen N. G., et.al. (2012) 'A wave generation toolbox for the open source cfd library: OpenFOAM', *International Journal for Numerical Methods in Fluids*,70, pp.1073–1088.

Higuera, P., et.al. (2013) 'Realistic Wave Generation and Active Wave Absorption for Navier–Stokes Models', *Coastal Engineering*, 71, pp. 102-18.

Menter, F.R. (1994) 'Two-equation eddy-viscosity turbulence models for engineering applications', *AIAA-Journal*, 32(8), pp. 269-289.

Hirt, C.W., and Nichols, B.D. (1981) 'Volume of fluid (VOF) method for the dynamics of free boundaries', *Journal of Computational Physics*, 39(1), pp. 201-225, ISSN 0021-9991, https://doi.org/10.1016/0021-9991(81)90145-5.

Devolder, B., et.al. (2017) 'Application of a buoyancy-modified k-ω SST turbulence model to simulate wave run-up around a monopile subjected to regular waves using OpenFOAM ®', *Coastal Engineering*, 125, pp. 81-94.

Issa, R.I. (1986) 'Solution of the Implicitly Discretised Fluid Flow Equations by Operator- Splitting', *Journal of Computational Physics*, 62, pp. 40-65, http://dx.doi.org/10.1016/0021-9991(86)90099-9.

WAFO-group (2000). 'WAFO - A Matlab Toolbox for Analysis of Random Waves and Loads -A Tutorial', Math*. Stat., Center for Math. Sci., Lund Univ., Lund, Sweden*, http://www.maths.lth.se/matstat/wafo.

Le Méhauté B. (1976) 'An Introduction to Hydrodynamics and Water Waves', *Springer*.

Baruah, G., et.al. (2022) 'Numerical Simulation of Nonlinear Wave Interaction with Floating Solar Platforms with Double Tubular Floaters Using Viscous Flow Model', *Proceedings of the ASME 2022 41st International Conference on Ocean, Offshore and Arctic Engineering OMAE2022 June 5-10, 2022, Hamburg, Germany*.

Parzen, E. (1962) 'On Estimation of a Probability Density Function and the Mode', *The Annals of Mathematical Statistics,* 33, pp 1065-1076, http://dx.doi.org/10.1214/aoms/1177704472.